Electronic Supplementary Material (ESI) for Nanoscale.
This journal is © The Royal Society of Chemistry 2016

Supporting Information: Enlightening the Ultrahigh Electrical Conductivities of Doped Double-Wall Carbon Nanotube Fibers by Raman Spectroscopy and First-Principles Calculations

Damien Tristant,[ab] Ahmed Zubair,[c] Pascal Puech,[*a] Frédéric Neumayer,[a]
Sébastien Moyano,[a] Robert J. Headrick,[def] Dmitri E. Tsentalovich,[def] Colin C. Young,[def]
Iann C. Gerber,[b] Matteo Pasquali,[def] Junichiro Kono,[cfg] and Jean Leotin[h]

This Supporting Information document presents additional DFT calculations, Raman spectroscopy experiments and analyses performed on high-conductivity double-wall carbon nanotube fibers as a function of temperature and current. In the first section, we study using *ab initio* calculations, the electronic properties between SO_3Cl molecules and metallic/semiconducting CNT, allowing us to use the equation (1) from the paper for our system. In the second section we describe the lattice temperature (T_L) dependence of the G-peak frequency, ω_G. A linear relationship between ω_G and T_L was found with a slope $d\omega_G/dT_L = -0.020 \pm 0.002\,\mathrm{cm^{-1}\cdot K^{-1}}$, which agrees with previous reports.[1] The third section deals with the temperature of a phonon system when the lattice is heated. The ratio between the anti-Stokes intensity, I_{AS}, and the Stokes intensity, I_S, allowed us to determine the thermal populations of phonons, which in turn yielded a photon temperature. The obtained phonon temperature agreed with the lattice temperature, confirming that phonons are in thermal equilibrium with the lattice (*i.e.*, there are no hot phonons). Finally, in the third section, we present and analyze Raman spectra for the double-wall carbon nanotube fiber at different currents from 0 to 80 mA. As the current increases, the G-band frequency, ω_G, decreases. The value of ω_G at each current can be associated with a lattice temperature through the linear $\omega_G - T_L$ relationship established in the first section. Specifically, we found that ΔT is equal to 135 K as the current increases form 0 to 80 mA.

[a] *CEMES-CNRS, UPR-8011, Université Fédérale de Toulouse-Midi-Pyrénées, 29 rue Jeanne Marvig, BP 94347 Toulouse, Cedex 4, France. Fax: +33 05 62 25 79 99; Tel: +33 05 67 52 43 57; E-mail: pascal.puech@cemes.fr*
[b] *LPCNO, UMR-5215 CNRS, INSA, Université Fédérale de Toulouse-Midi-Pyrénées, Université de Toulouse, 135 Avenue de Rangueil, 31077 Toulouse, France.*
[c] *Department of Electrical and Computer Engineering, Rice University, 6100 Main St., Houston, Texas 77005, USA.*
[d] *Department of Chemical and Biomolecular Engineering, Rice University, 6100 Main St., Houston, Texas 77005, USA.*
[e] *Department of Chemistry, Rice University, 6100 Main St., Houston, Texas 77005, USA.*
[f] *Department of Materials Science and NanoEngineering, Rice University, 6100 Main St., Houston, Texas 77005, USA.*
[g] *Department of Physics and Astronomy, Rice University, 6100 Main St., Houston, Texas 77005, USA.*
[h] *LNCMI-CNRS, UPR 3228, Université Fédérale de Toulouse-Midi-Pyrénées, 143 avenue de Rangueil, 31400 Toulouse, France.*

1 Fermi level dependent electron doping level in metallic/semiconducting single-wall carbon nanotubes

To support our arguments on the dependence between the Fermi level shift and the hole charge transfer per carbon atom, we studied *via* the DFT calculations, the effects of electron transfer between SO_3Cl molecules and metallic/semiconducting carbon nanotube. In order to determine the effects of the SO_3Cl concentration, several unit cells containing 132 to 200 carbon atoms in interaction with molecules are considered. Here we use $(1\times1\times5)$, $(1\times1\times3)$, $(1\times1\times3)$ and $(1\times1\times2)$ primitive cells of (7,7), (11,0), (14,14) and (25,0) CNT respectively. For smaller diameters, only one molecule is adsorbed, while for the two largest diameters, the number of adsorbed molecules is equal to 1, 2 and 12. For example, 7 SO_3Cl molecules is taken as reference for the maximum coverage value, that is 100%, for the (7,7) and (11,0) tubes, while 12 molecules for the (14,14) and (25,0) tubes. Figure 1 illustrates a coverage value of 8.3% for both (14,14) and (25,0) tubes.

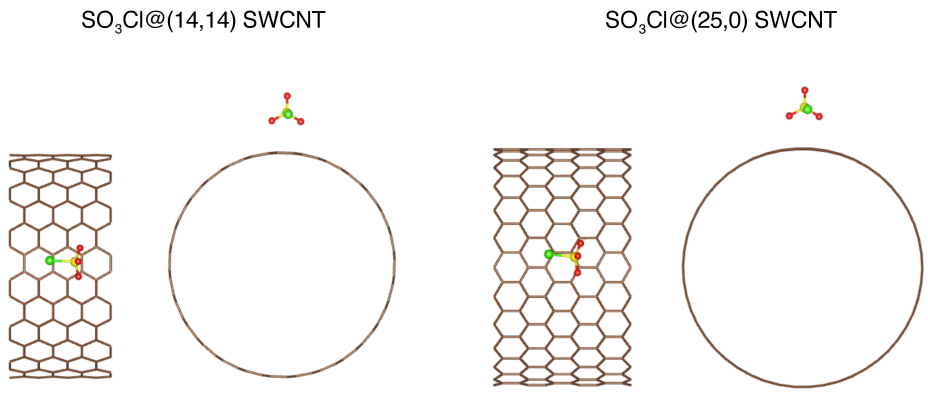

Figure 1 (Color online) View of the adsorption site of SO_3Cl molecule on: a (14,14) metallic armchair SWCNT (left panel) and a (25,0) semiconducting zigzag SWCNT (right panel), after geometry relaxation.

The effects of electron transfer between the two subsystems on the electronic structure properties of the (14,14) and (25,0) CNT are shown in Fig. 2 and 3 respectively. From the band structure and the DOS, it is clear that the molecule is physisorbed and the Fermi level is shifted around 0.31 eV for both systems, corresponding to an electronic transfer from the substrat to the molecule. For each systems, the E_1^{M} and E_1^{SC} energy, the hole charge transfer per carbon atom f_{c}, the Fermi energy shift ΔE_{F}, the result of equation (1) from the paper and the error rate between ΔE_{F} and the value of eqn (1) are reported in Table 1. As we can see, the calculated values E_1^{M} and E_1^{SC} (half of the optical transition energy) for a doped (14,14) and (25,0) tube respectively decrease with further increase in the doping level. These results are consistent with the previous reports.[2] We also observe, for large diameters, that the error rate decreases as the charge transfer increases. This means that eqn (1) in the paper, for our system, is an excellent approximation.

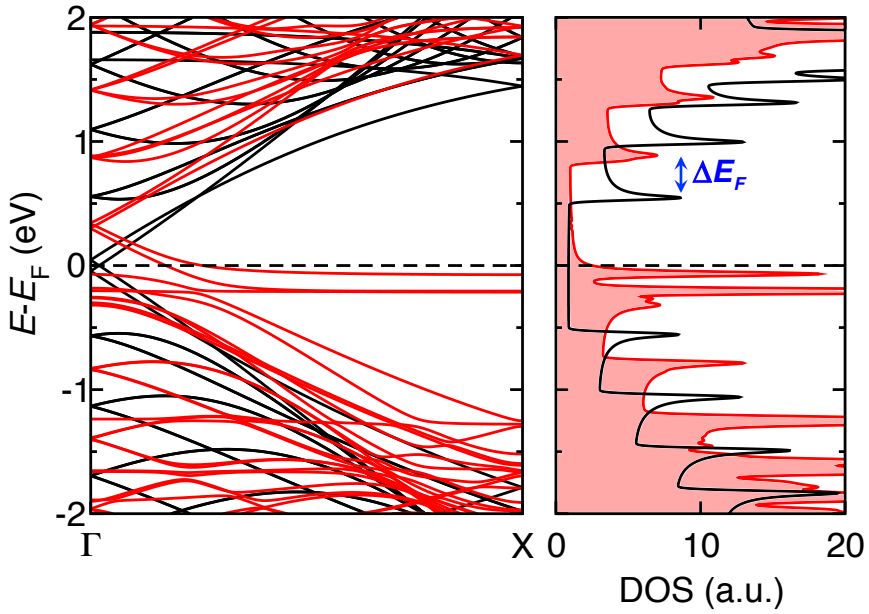

Figure 2 (Color online) Calculated electronic band dispersions and density of states of the isolated (14,14) metallic armchair SWCNT (black line) and with SO_3Cl molecule adsorbed on SWCNT (red line) at low SO_3Cl concentration (0.60 %). The Fermi level is at zero energy. When it is doped, the Fermi level ΔE_F is shifted to around 0.31 eV.

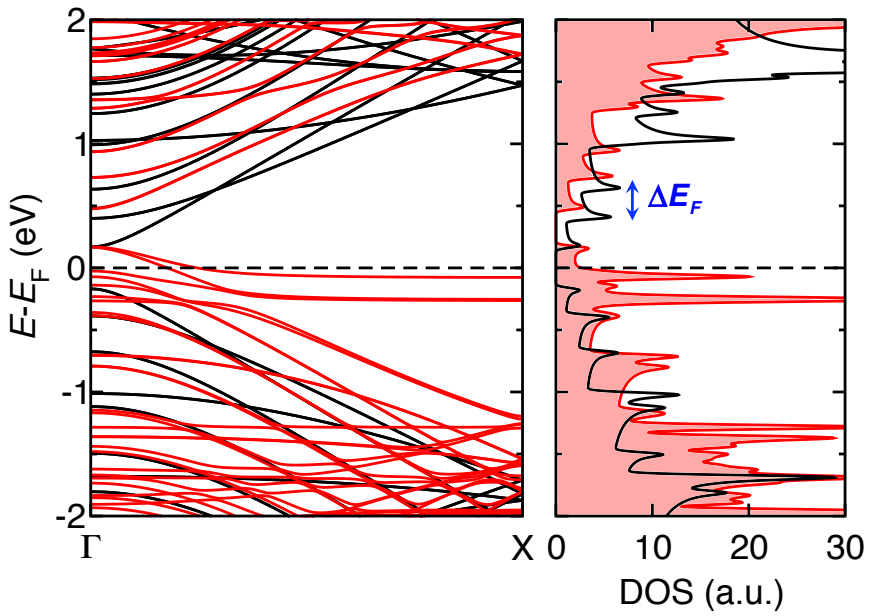

Figure 3 (Color online) Calculated electronic band dispersions and density of states of the isolated (25,0) semiconducting zigzag SWCNT (black line) and with SO_3Cl molecule adsorbed on SWCNT (red line) at low SO_3Cl concentration (0.50 %). The Fermi level is at zero energy. When it is doped, the Fermi level ΔE_F is shifted to around 0.31 eV.

Table 1 Diameter (nm), E_1^{M} and E_1^{SC} energy (eV), the hole charge transfer per carbon atom f_{c}, the Fermi energy shift ΔE_{F} (eV), the result of eqn (1) from the paper (eV) and the error rate between ΔE_{F} (%) and the value of eqn (1), as a function of the SO_3Cl coverage value (%) deposited on metallic (M) and semiconducting (SC) CNT.

CNT	SO_3Cl coverage	Diameter	E_1^{M}	E_1^{SC}	f_{c}	ΔE_{F}	$6.04\sqrt{f_{\mathrm{c}}}$	Error rate
(7,7)	13.8%	0.95	0.97		0.0060	0.27	0.47	43%
(11,0)	14.6%	0.86		0.47	0.0062	0.47	0.48	2%
(14,14)	8.3%	1.90	0.56		0.0043	0.31	0.40	23%
	16.7%	1.90	0.54		0.0082	0.55	0.55	0%
	25%	1.90	0.53		0.0121	0.62	0.66	6%
	100%	1.90	0.52		0.0329	1.07	1.09	2%
(25,0)	8.3%	1.96		0.18	0.0038	0.31	0.37	16%
	16.7%	1.96		0.16	0.0074	0.49	0.52	6%
	25%	1.96		0.16	0.0106	0.64	0.62	3%
	100%	1.96		0.15	0.0358	1.19	1.14	4%

2 Temperature Dependence of the *G*-Peak Frequency

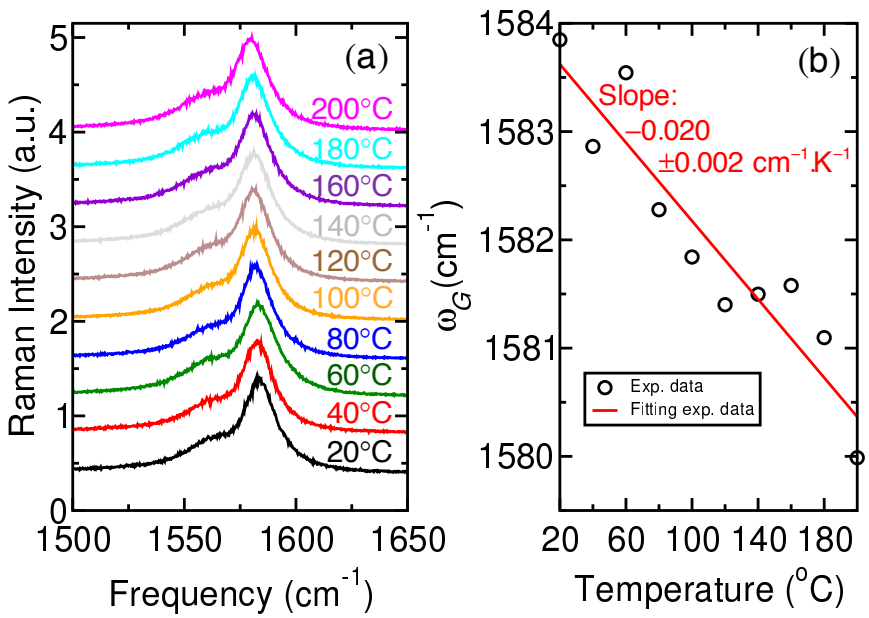

Figure 4 (Color online) (a) Raman spectra of a double-wall carbon nanotube fiber at various lattice temperatures, T_{L}, between 20 and 200°C in the *G*-band range in the Stokes domain. The spectra are vertically offset for clarity. (b) Raman shift frequency of the *G*-peak, ω_G, versus lattice temperature, T_{L}. Data are fit with a linear function with slope $\mathrm{d}\omega_G/\mathrm{d}T_{\mathrm{L}} = -0.020 \pm 0.002\,\mathrm{cm}^{-1}\cdot\mathrm{K}^{-1}$ (red solid line).

Figure 4(a) shows Raman spectra of the *G*-band component for a double-wall carbon nanotube fiber at various lattice temperatures, T_{L}, from 20°C to 200°C. As T_{L} increases, the *G*-band frequency, ω_G, decreases. The observed ω_G is plotted as a function of T_{L} in Figure 4(b). The data can be fit with a straight line (red solid line) with a slope $\mathrm{d}\omega_G/\mathrm{d}T_{\mathrm{L}} = -0.020 \pm 0.002\ \mathrm{cm}^{-1}\cdot\mathrm{K}^{-1}$, which is consistent with a previous report.[1]

3 Determination of the Phonon Temperature from the Anti-Stokes-to-Stokes Intensity Ratio

Figure 5 shows G-band Raman spectra for the double-wall carbon nanotube fiber, both in the anti-Stokes (left) and Stokes (right) domains, at $T_L = 60$, 90 and 160°C. For better visibility, the spectra in the anti-Stokes domain are multiplied by a factor of 100. The intensity and width of the peak in the anti-Stokes domain rapidly grow as T_L increases. The ratio between the anti-Stokes intensity, I_{AS}, and the Stokes intensity, I_S, allows one to obtain information on the thermal populations of phonons. This is because, in the anti-Stokes process, a phonon that is already present is annihilated and transfers its energy to the incoming photon. Its intensity is proportional to the initial phonon population, contrary to the Stokes process, in which a new phonon is created.

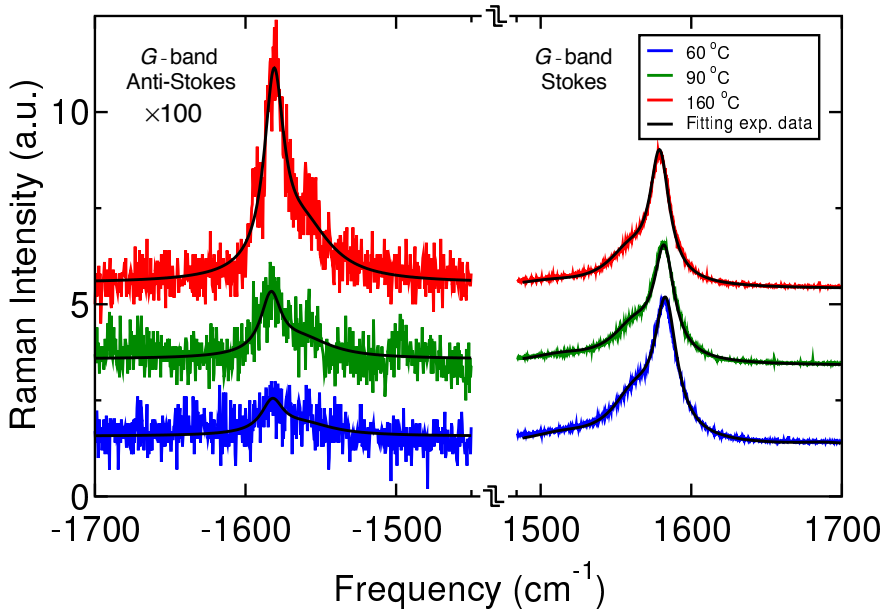

Figure 5 (Color online) Anti-Stokes (left panel) and Stokes (right panel) G-band Raman spectra of a DWCNT fiber at lattice temperatures of 60, 90 and 160°C. For better visibility, the anti-Stokes spectra are multiplied by a factor of 100. Each spectrum is fit by one constant baseline and two Lorentzian functions (black solid lines).

Specifically, by comparing the anti-Stokes-to-Stokes intensity ratio, I_{AS}/I_S, at two different lattice temperatures, $T_{L,1} = T_0$ and $T_{L,2} = T_0 + \Delta T_L$, one can determine the temperature increase in the phonon system between the two situations. Assuming Bose-Einstein statistics, one can write the phonon temperature increase as

$$\Delta T_{S/AS} = \frac{1}{\frac{1}{T_0} - \frac{k_B}{E_{phonon}} \ln\left(\frac{(I_{AS}/I_S)_{T_0+\Delta T_L}}{(I_{AS}/I_S)_{T_0}}\right)}, \tag{1}$$

where E_{phonon} is the phonon energy of the G-band and k_B is the Boltzmann constant. Note that we assumed that the ΔE_{ii} effect is negligible (no change in the modulation of the electronic susceptibility by the atomic displacement).

Using Eq. (1), we found that $\Delta T_{S/AS} = (108 \pm 15)$°C when $\Delta T_L = 160°C - 60°C = 100°C$ and that $\Delta T_{S/AS} = (68 \pm 15)$°C when $\Delta T_L = 160°C - 90°C = 70°C$. Therefore, we can conclude that $\Delta T_{S/AS} = \Delta T_L$, that is, the phonon temperature deduced from Eq. (1) agrees with the lattice temperature deduced from the G-peak frequency.

4 Temperature of a Current-Driven Fiber

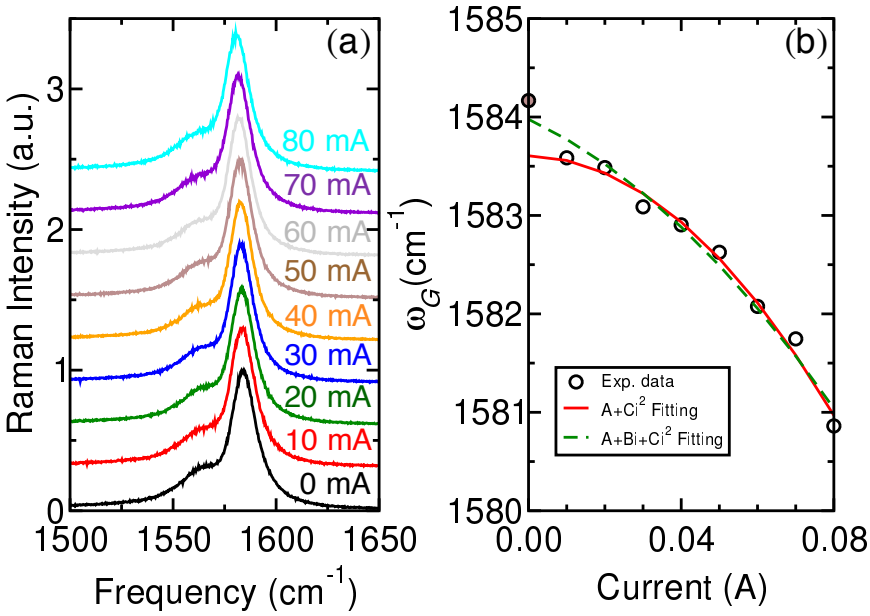

Figure 6 (Color online) (a) Raman spectra of the *G* mode for a current-driven double-wall carbon nanotube fiber. The panel, shifted for clarity, shows the evolution of the *G*-mode in the Stokes domain at currents from 0 to 80 mA. (b) Raman shift of the *G*-band Stokes line versus current. Data are fit with a quadratic function, with (green dashed line) and without (red full line) the first value at 0 mA.

Figure 6(a) shows *G*-band Raman spectra for the double-wall carbon nanotube fiber at different currents from 0 to 80 mA. As the current increases, the *G*-band frequency, ω_G, decreases, which are summarized in Figure 6(b). We observe a quadratic behavior of the current. This result is consistent with the study of current carrying capacity of double-wall carbon nanotube fibers.[3] The frequency, ω_G, at each current can be associated with a temperature through the linear relationship established in Figure 4(b), *i.e.*, $d\omega_G/dT_L = -0.020 \pm 0.002$ cm^{-1}·K^{-1}. Specifically, we find that $\Delta T(\omega_G)$ is equal to 135 K as the current increases form 0 to 80 mA.

5 RBMs versus temperature

Raman spectra recorded for an undoped DWCNT fiber are shown in Figure 7. Around 200 cm^{-1}, there is a gap in the RBM signal. It is clear that the RBM intensity in the 200 to 300 cm^{-1} range is more sensitive to temperature. After integrating the Raman intensity between 100 to 200 cm^{-1} (I_1) and 200 to 300 cm^{-1} (I_2) and calculating the ratio I_1/I_2, we obtained a way to estimate the temperature. We tried to follow one RBM but failed. Several problems were present. While the temperature is changed, the setup slightly moves, and as a result, we do not observe exactly the same point. Thus, the RBM decomposition is not the same, and only a time consuming statistical analysis could fix this point. A family of modes is present, and the intensity of each mode is affected by the temperature differently (energy between the laser and the transition). As the modes are not resolved and the temperature shift of the RBM reported in the literature is not constant for all chiralities[4], decomposition is not straightforward. Due to these effects, using the RBM with fibers remains a challenge.

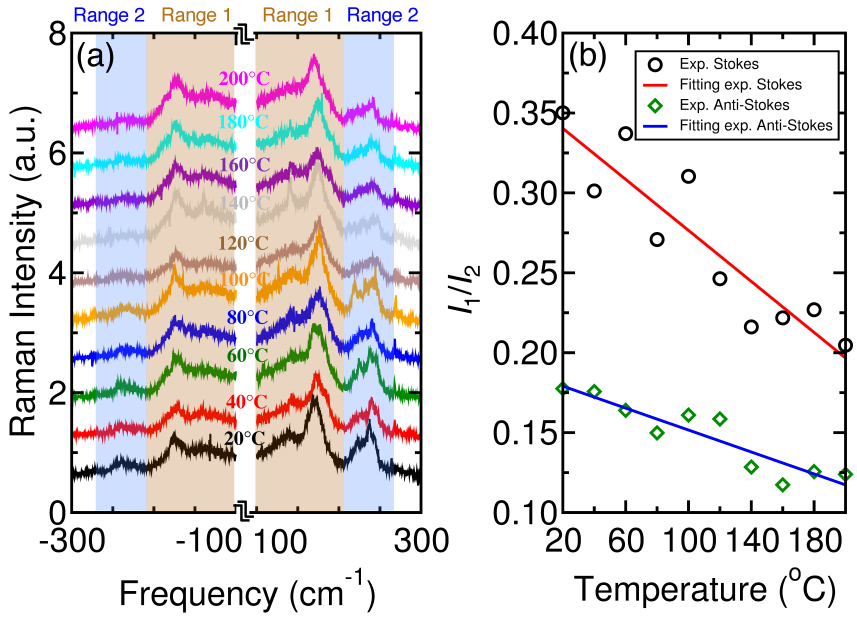

Figure 7 (Color online) (a) Raman spectra of the RBMs range versus temperature and (b) ratio of the integrated intensities I_1/I_2 corresponding to the range 1 and 2 versus temperature.

6 RBMs versus current

Raman spectra recorded for an undoped DWCNT fiber are shown in Figure 8. Using the same method as for temperature dependence, we plot the ratio I_1/I_2. At a value of 80 mA, the temperature increase is 150±50 K.

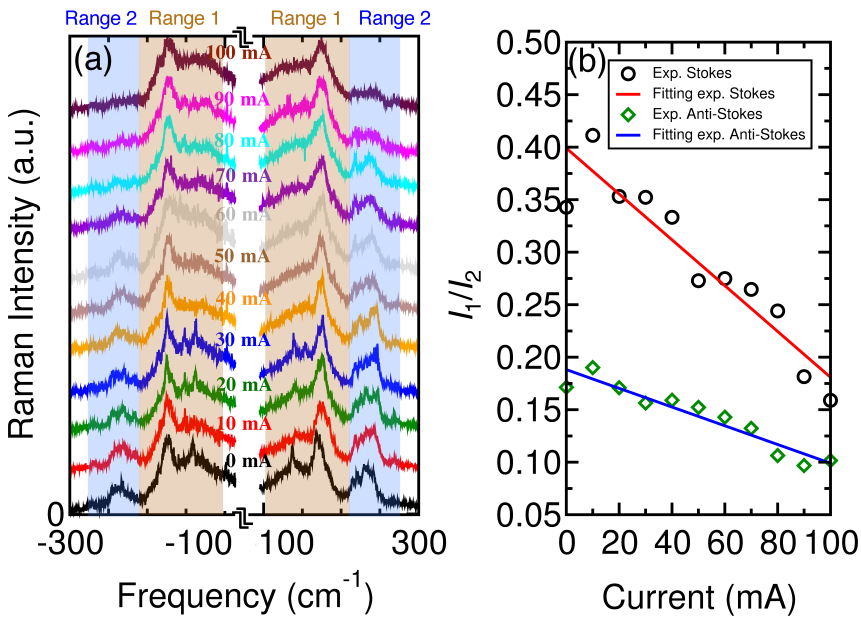

Figure 8 (Color online) (a) Raman spectra of the RBMs range versus current and (b) ratio of the integrated intensities I_1/I_2 corresponding to the range 1 and 2 versus temperature.

References

[1] M. Steiner, M. Freitag, V. Perebeinos, J. C. Tsang, J. P. Small, M. Kinoshita, D. Yuan, J. Liu and P. Avouris, *Nature Nanotech.*, 2009, **4**, 320–324.

[2] L.-C. Yin, H.-M. Cheng, R. Saito and M. S. Dresselhaus, *Carbon*, 2011, **49**, 4774–4780.

[3] X. Wang, N. Behabtu, C. C. Young, D. E. Tsentalovich, M. Pasquali and J. Kono, *Adv. Funct. Mater.*, 2014, **24**, 3241–3249.

[4] N. R. Raravikar, P. Keblinski, A. M. Rao, M. S. Dresselhaus, L. S. Schadler and P. M. Ajayan, *Physical Review B*, 2002, **66**, 235424.